Blistering of Industrial Floor on Concrete Substrate: the Role of the Air Overpressure

S.V. Aher[1], P. Devillers[*2], G. Fau[3], B. Tranain[3] and C. Buisson[2]
[1]Department of Civil Engineering, Indian Institute of Technology Kanpur, India, [2]Centre des Matériaux de Grande Diffusion, Ecole des Mines d'Alès, France, [3]Centre Scientifique et Technique du Bâtiment, Champs sur Marne, France
*Corresponding author: Centre des Matériaux de Grande Diffusion, Ecole des Mines d'Alès, 6 avenue de Clavières, 30 319 Alès cedex, France, Philippe.Devillers@mines-ales.fr

Abstract: A three dimensional COMSOL Multiphysics, transient analysis, diffusion model has been adopted to model the transfers of water in the industrial concrete floors. To take into account the different initial saturation levels at the different levels of the slab, the model is divided into three subdomains. The rise of the waterfront is also simulated and the air overpressure thereby developed at the interface is calculated. Comparison of numeric simulations with tests realized in laboratory throw some light on the role of the capillary pressure in the pressure developed in the concrete/cover interface.

Keywords: blistering, capillary pressure, diffusivity, air pressure.

1. Introduction

Surface coating can fulfill their function satisfactorily over an extended period of time only if there is a good bond between the concrete substrate and the coating. The most numerous cases of blistering affect the airtight covers of the concrete subjected to negative pressures of humidity from the support. The general objective of this study is the understanding of the blistering phenomenon. In the literature, the first evoked cause is the rise of water by capillarity in the concrete which will compress the air situated above and generate an air overpressure [1]. The migration of the water in the hardened concrete is made by capillary action. When the under face of the slab is in touch with some water, the concrete quickly stuffs itself with water, then the liquid/gas interface moves upward by compressing the air situated above the interface. The air pressure grows strongly when the material is close to the saturation. Comparison of numeric simulations realized with COMSOL Multiphysics with tests realized in laboratory throw some light on the role of the capillary pressure in the pressure developed in the concrete/cover interface.

2. Governing equations

The three big hypotheses which intervene in this model are: a rigid solid matrix, the existence of three phases (liquid, gas and solid) and the choice of the gradients of fluids pressure as the main driving terms to describe the impulse of these fluids [2]. The equations of mass conservation of the fluid are expressed by means of the averaged sizes [3].

For the concrete, the mass balance equations of air, water vapor and liquid water are respectively :

$$\frac{\partial\langle\rho_a\rangle}{\partial t} + \nabla.\left(\langle\rho_a\rangle^g\langle\overrightarrow{V_a}\rangle\right) = 0$$

$$\frac{\partial\langle\rho_v\rangle}{\partial t} + \nabla.\left(\langle\rho_v\rangle^g\langle\overrightarrow{V_v}\rangle\right) = K$$

$$\frac{\partial\langle\rho_l\rangle}{\partial t} + \nabla.\left(\langle\rho_l\rangle^l\langle\overrightarrow{V_l}\rangle\right) = -K$$

Where $\rho_i$and $\langle\overrightarrow{V_i}\rangle$ are respectively, the density and the velocity of the constituent *i*, and *K* is the rate of evaporation of water. The water content *w* is defined by :

$$w = \frac{\langle\rho_l\rangle + \langle\rho_v\rangle}{\langle\rho_s\rangle}$$

By adding the mass balance equations of water vapor and liquid water, we get :

$$\rho_s\frac{\partial\langle w\rangle}{\partial t} = -\nabla.\left(\langle\rho_v\rangle^g\langle\overrightarrow{V_v}\rangle + \langle\rho_l\rangle^l\langle\overrightarrow{V_l}\rangle\right)$$

Mainguy et al. [4] showed that the main part of the transport is made by liquid water. During the natural drying, for example, we have evaporation of the liquid water in the superficial zone of concrete which leads to a gradient of liquid water between the surface and the core, as well as to a water flow towards the outside until the balance is reached between the external and internal hydric states. Thus, the water transport is mainly due to the filtration of the liquid phase. The vapor flow, and the term of phase change

are insignificant. The free water flow is then given by the generalized Darcy law :

$$\langle\rho_l\rangle^l\langle\overrightarrow{V_l}\rangle = -\langle\rho_l\rangle^l \frac{k k_{rl}}{\mu_l}(\nabla\langle p_l\rangle^l - \langle\rho_l\rangle^l\,\vec{g})$$

Where k is the intrinsic permeability of the medium (to be determined experimentally), k_{rl} the relative permeability with respect to water and μ_l is the dynamic viscosity of water. Several correlations, as a function of the saturation degree, are given in the literature for k_{rl} which can be also defined by the adjustment of experimental profiles of water content. The pressure difference p_c in the interface between the gaseous phase and the liquid phase is called capillary pressure; it is a measurable size within the porous medium and, it evolves according to the saturation degree :

$$p_c = \langle p_g\rangle^g - \langle p_l\rangle^l$$

Under the hypothesis that the pressure of the gaseous phase is uniform and constant and that the gravity effects are insignificant, the generalized Darcy law becomes :

$$\langle\rho_l\rangle^l\langle\overrightarrow{V_l}\rangle = \langle\rho_l\rangle^l \frac{k k_{rl}}{\mu_l}(\nabla \mathrm{p_c})$$

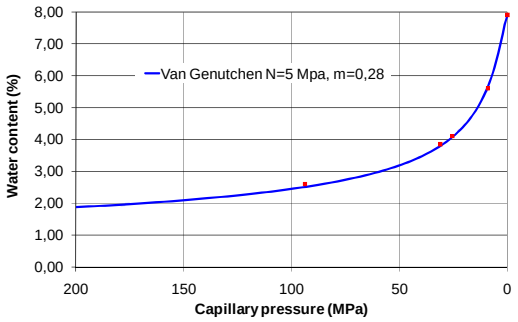

Figure 1. Sorption isotherm of reference concrete.

In isothermal conditions, in the thermodynamics balance, the isotherm of adsorption or of desorption allows to connect the capillary pressure and the water content w (figure 1). In figure 1, the red points correspond to experimental data obtained on a reference concrete of the laboratory. Concrete disks, preconditioned at a relative humidity of 50 % were placed in desiccators containing saturated salt solutions assuring different relative humidity. The principle of the experimental study is to realize successive and regular weightings of concrete disks to establish the kinetics of adsorption. The water contents in the balance according to the relative humidity, allow us to obtain the isotherm of adsorption. This relation can be modeled by the equation proposed by Van Genutchen [5] for soil (figure 1) :

$$p_c = N\left(\left(\frac{w}{w_{sat}}\right)^{\left(-\frac{1}{m}\right)} - 1\right)^{(1-m)}$$

This allows us to write the generalized Darcy law in the form :

$$\langle\rho_l\rangle^l\langle\overrightarrow{V_l}\rangle = \langle\rho_l\rangle^l \frac{k k_{rl}}{\mu_l}\left(\frac{\mathrm{dp_c}}{\mathrm{dw}}\nabla \mathrm{w}\right)$$

Under these hypotheses, the equation of mass conservation is transformed into an equation of diffusion type :

$$\rho_s \frac{\partial\langle w\rangle}{\partial t} = \nabla.\left(\langle\rho_l\rangle^l \frac{k k_{rl}}{\mu_l}\left(\frac{\mathrm{dp_c}}{\mathrm{dw}}\nabla \mathrm{w}\right)\right)$$

This equation can then be represented as :

$$\frac{\partial\langle w\rangle}{\partial t} = \nabla.(D(w)\nabla \mathrm{w})$$

The hydraulic diffusivity $D(w)$ is an apparent diffusivity which varies in a very non linear manner with water content, becoming very low when the water content decreases. The non linearity of the hydraulic diffusivity results from water content/capillary pressure relationship on one hand and the water content/relative permeability with respect to water relationship on the other hand. The wedging of the relation $D(w)$ can be made by using a curve of mass loss. Except on the control of the limiting conditions, this experiment does not present difficulty as long as it is on a laboratory sample.

3. Materials and methods

A composite cement CEM II/B-M (LL-S) 42.5 R CE was used for the entire experimental campaign. The aggregates used were of type calcareous, recomposed sand (0/4 mm) and crushed gravels (6.3/14 mm and 14/20 mm). Water-reducing plasticizer was also used. The effective water cement ratio was 0.6 and the gravel/sand ratio was 1.11. The workability criterion selected for the reference concrete was: a slump of 15 ± 3cm from Abrams cone test. Table 1 gives the mixture proportion of the reference concrete.

Slabs of cross-section 0.35m x 0.35m and height of 0.062 m were realized. The concrete was placed in the moulds by vibration. Three hygrometers were placed at three different

heights to check the relative humidity and temperature inside the concrete slab (figure 2).

Figure 2. Instrumentation of the slab.

Table 1: Concrete mixture proportion

Cement CEM II/B 42.5 R	320 kg
Gravel 14/20	575 kg
Gravel 6.3/14	340 kg
Sand 0/4	825 kg
Plasticizer	0.960 kg
Water	210 kg

The compressive strength of concrete was measured at 28 days on three cubes (150 mm sized) according to the NF EN 12390-3 standard. The mean compressive strength is 39.4 ± 0.2 MPa.

The water opened porosity and apparent specific weight were measured on cubic samples (70 mm sized), extracted from cylindrical mould samples, according to the French AFPC-AFREM standard: vacuum water saturation, hydrostatic weight and drying at 105±5°C until constant mass. The water opened porosity is well correlated with the compressive strength of concrete. The water open porosity of the reference concrete is 17.4 ± 0.33 % and the apparent specific weight is 2200 ± 10 kg/m^3. The saturation water content w_{sat} is thus 7.9 %.

3. Use of COMSOL Multiphysics

A three dimensional COMSOL Multiphysics, transient analysis, diffusion model has been adopted to model the transfers of humidity in the industrial concrete floors. The chosen dimensions of the slab are 35 cm x 35 cm x 6.2 cm (figure 3). Experimentally, it is very difficult to achieve the same initial relative humidity throughout the slab. Indeed, when the water concentrations differ only by 10%, the kinetics of water transfer become very slow. As a result, the concentrations inside the slab do not become uniform throughout, even after a long period. In the test that we carried on, we placed three hygrometers at three different heights inside the slab (figure 2 and 3). The hygrometers used in the test were 6 mm in diameter, which is a significant dimension in a 6.2 cm high slab. Assuming that the rising water is immediately detected by the hygrometer as soon as it first comes in contact with the bottom of the hygrometer, the three subdomains are defined such that the neighboring two subdomains abut at a location at the midpoint of the bottom of the two hygrometers.

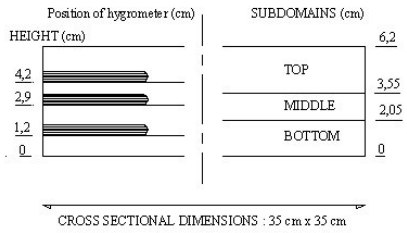

Figure 3. Geometry of the model.

Figure 4 gives the evolution of the hygrometry, with the time, of a reference concrete slab released from the mould after 14 days and put in endogenous conditions after 85 days. We notice that in spite of a phase of humidity redistribution of about 100 days, there is still a difference of 5 % hygrometry inside the slab. As during experimental campaign, the phase of humidity redistribution will be only of 7 days, the hygrometry gradients inside the slab will be much more important.

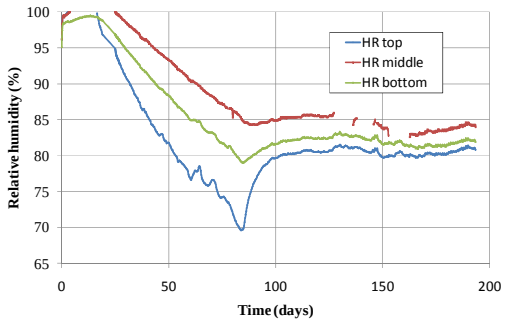

Figure 4. Preconditioning of the slab.

To take into account the different initial saturation levels at the different levels of the slab, the model is then divided into three subdomains (figure 3). As we had three sets of data, we could assign these initial conditions to the respective subdomains. In the slab, the initial relative humidity measured at the location of the top hygrometer is 65%, at the middle hygrometer, it is 78.5% and at the bottom hygrometer, it is 74%. Using the Van Genutchen's law, these correspond to initial water contents of 3.1, 3.8 and 3.5 % respectively.

The base of the slab is subject to a constant water content of 7.9 %. All other faces are insulated. Continuity equation is applied at the interior boundaries between the three subdomains.

An exponential law to describe the variations of the hydraulic diffusivity $D(\theta)$ with the reduced water content θ is often used [6] :

$D(\theta) = D_0 exp^{(n\theta)}$

Where D_0 and n are empirically-fitted constants. The hydraulic diffusivity of many common building materials has been found to obey the exponential law with n being between 6 and 8 and varying little between materials. θ is the reduced water content, scaled to be zero and one for the initial and saturated water contents, w_i and w_{sat}, respectively:

$$\theta = \frac{w - w_i}{w_{sat} - w_i}$$

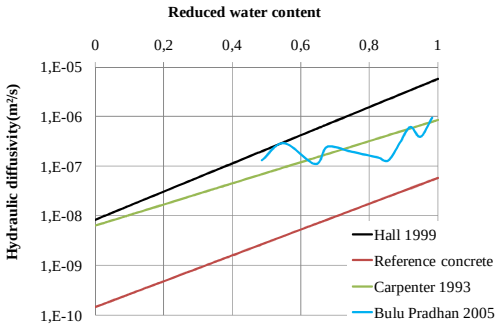

Figure 5. Hydraulic diffusivity as a function of reduced water content.

Figure 5 gives examples of the variation of hydraulic diffusivities with reduced water content found in the literature [6]. In this figure the variation of the hydraulic diffusivity of the reference concrete is also presented (D_0=1.45x10^{-10} m²/s and n =5.97).

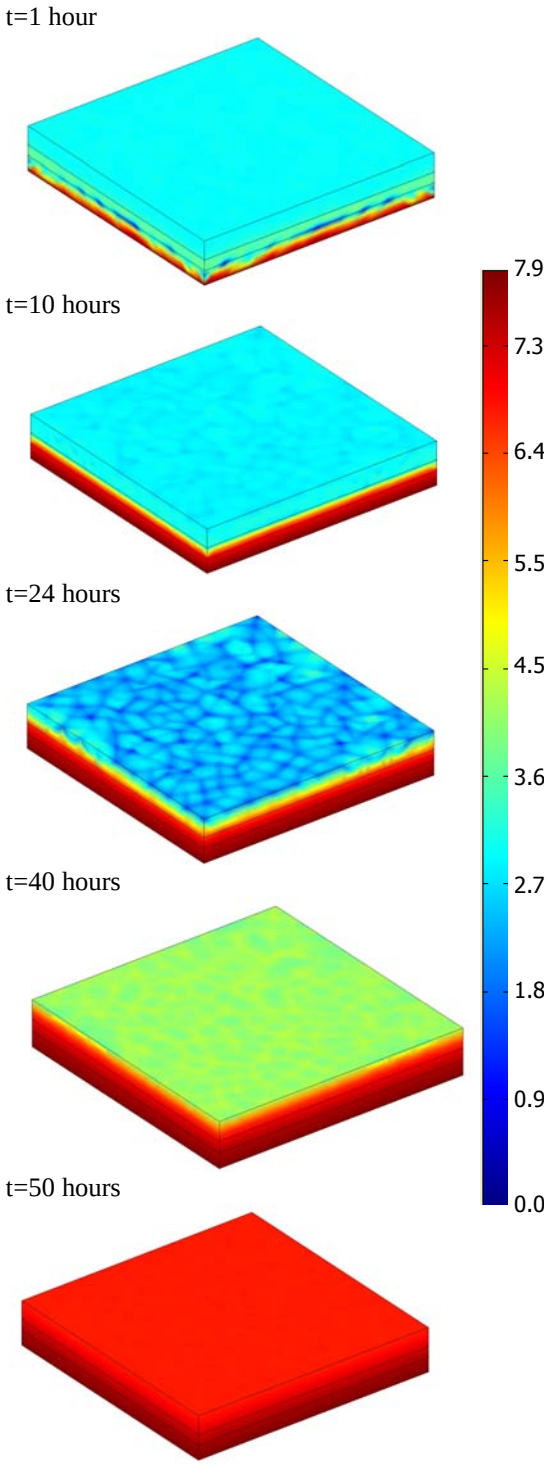

Figure 6. COMSOL Multiphysics results.

Time scale is 75 hours, with the time interval of 0.5 hours. As time passes by, the unsaturated concrete slab absorbs water till it gets completely saturated (figure 6). The bottom part of the slab saturates first. After two hours, the relative humidity there becomes greater than 95%. The middle part starts to absorb water after six hours and the relative humidity here becomes greater than 95% only after 12 hours. The top part of the slab starts to absorb water after ten hours. We notice that the low part of the material quickly stuffs itself with water. We can consider that the concrete is saturated after 75 hours.

One of the objectives of the study is to know the movement of the liquid/gas interface. We consider that this front has reached a given level in the slab only when the relative humidity at this level becomes higher than 98 %. The Comsol Multiphysics 3.2 software is able to supply numerical values indicating the liquid/gas front displacement as a function of time (figure 7). After exploitation of these values, the evolution of the front with respect to time can be drawn.

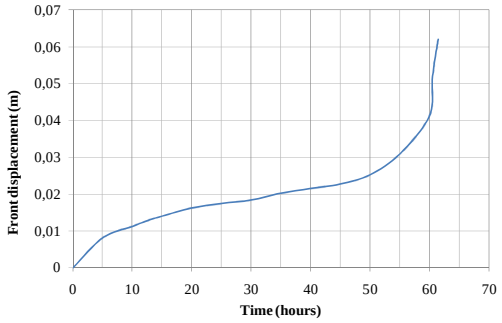

Figure 7. Front displacement as a function of time.

The air overpressure can then be calculated supposing that air behaves as an ideal gas :

$$\frac{\langle P_a \rangle^g}{\langle \rho_a \rangle^g} = \frac{RT}{M_a}$$

Where $\langle P_a \rangle^g$ is the air pressure inside the material (Pa), $\langle \rho_a \rangle^g$ the air density (kg/m^3), R the ideal gas constant (8307 J/K/mol), T the air temperature (283 K) and, M_a the molar mass of air (28.2 g/mol).

We know that $\langle \rho_a \rangle^g$ varies as a function of the humidity movements inside concrete according to:

$$\langle \rho_a \rangle^g = \frac{m_a}{V_g}$$

Where m_a is the initial air mass in the concrete slab and V_g is the volume of the voids occupied by the air above the liquid/gas front. The mass of air initially present in the material is calculated from the porosity of the reference concrete, the volume of the concrete slab V and the mean saturation rate at the starting of the test S_{ri}, as:

$$m_a = \langle \rho_a \rangle^g \, n \, S_{ri} \, V$$

We can then draw the evolution of the air overpressure in the concrete as a function of time. In figure 8, we notice that after 25 hours of capillary rise, there is an overpressure of about 0.4 bar under the cover. This overpressure grows strongly after 60 hours to exceed 1 MPa after 61 hours.

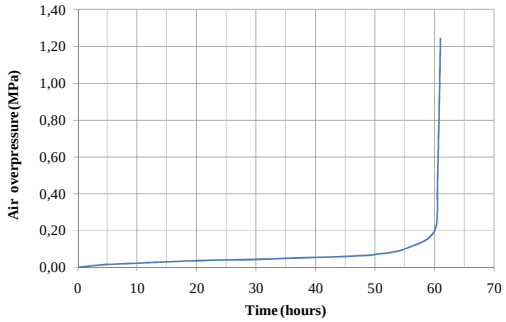

Figure 8. Air pressure as a function of time.

4. Experimental results

After casting, the upper surface of the slab is protected from desiccation with a plastic film. The slab is released from the mould after 14 days. The lateral surfaces of the slab are coated with resin and aluminum sheet (figure 9). After 28 days the concrete slab is preliminary dried at 60°C for 7 days, then put in air tight bags and placed in an air conditioned room for 7 days at 10°C. To measure the air overpressure due to the rise of water by capillarity, a steel plate provided with a pressure sensor is stuck on the upper face of the slab before starting the test (figure 9).

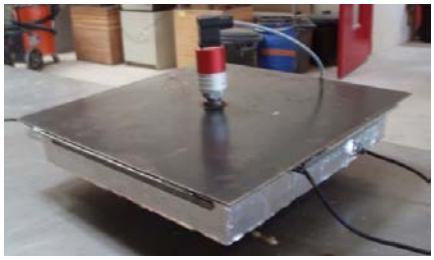

Figure 9. Instrumentation of the slab.

The test consists in immersing the base (the first ten millimetres) of the concrete slab in water at 10°C. The tests carried out during this study show that the concrete slab is saturated after 95 hours. Figure 10 gives the results of this test. In this figure, the dotted lines represent the experimental values, the full lines the numerical simulations realized with COMSOL Multiphysics.

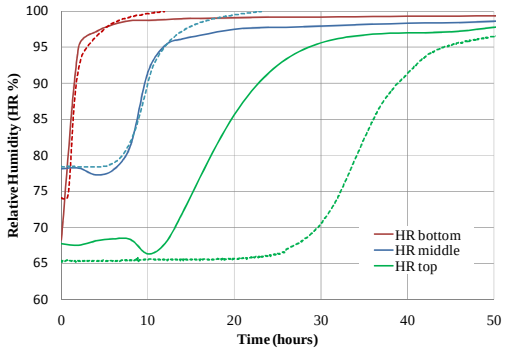

Figure 10. Experimental results.

We can see that for relative humidity higher than 95%, the curves are highly non linear. We notice that for the first two hygrometers, the experimental measures match well to the numeric simulations for relative humidity lesser than 95 %. On the other hand, for the third hygrometer there is a gap between the experimental values and the numeric simulations. Experimentally, the absorption of water starts with a delay of about fifteen hours as compared to the numeric simulations

In spite of all the precautions taken to assure the air tightness of the pressure sensor and the steel plate, we registered no increase of the air pressure.

5. Discussion

In the imbibition experiment, under the influence of slowly decreasing capillary pressure, the liquid water may substitute for the air initially present in pores of increasing diameter. In the earlier stages of the process, only a small part of the porous distribution is potentially accessible to the liquid water. But, as the capillary pressure decreases, the potentially accessible porous volume increases; a cluster of accessible pores develop between them new connections, and they group together in a cluster of bigger extension, thereby simultaneously increasing the thickness of the region effectively contaminated by the imbibition.

Simultaneously, another phenomenon appears, and gains importance - the trapping of air. Indeed, so that the liquid water can substitute for the air in a potentially accessible region, two conditions are required. The considered region must be connected in face of injection by the infinite cluster beforehand of the invasion. And, so that the air can be expelled, it is also necessary that this region is connected to the outside by a continuous domain still occupied by air.

Now as the imbibition progresses, the remaining volume occupied by air is reduced and it splits. Isolated regions still not invaded by liquid water appear, until the break of the connection of the gaseous phase. The air contained in pores cluster which was isolated during the imbibition is definitively trapped.

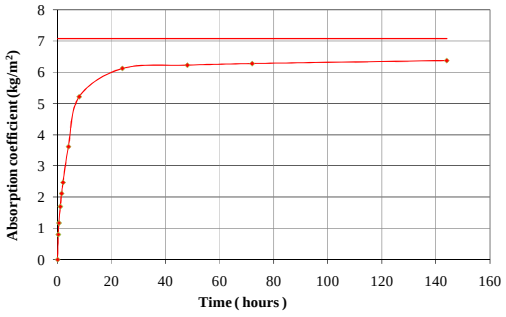

Figure 11 : Capillary absorption.

In order to study this phenomenon, capillary adsorption tests have been made on the reference concrete. The three samples are preliminary dried at 80°C until constant mass, then put in air-

tight bags and placed in a drying room for 10 days. The lateral surfaces of samples are coated with resin. The test consists in immersing the base (the first three millimetres) of the cylindrical concrete samples (diameter 110 mm, high 40 mm) in water. The tests carried out during this study show that the value of the capillary adsorption coefficient is 6.12 kg/m² at 24 hours and 6.37 kg/m² at 144 hours (figure 11). The theoretical adsorption coefficient of the reference concrete is 7.07 kg/m². That means that at the end of the test the saturation degree of the reference concrete is 90.2 % for samples 40 mm high. Indeed, the residual saturation depends on the size of the sample because the isolation of the pockets of air is less important near the face of release.

6. Conclusion

This study shows that the rise of water by capillarity in coated concrete floors does not drive to the development of an air overpressure in the concrete/cover interface. According to the theory, the air overpressure becomes important only when the liquid/gas interface gets closer to the coated surface of concrete (figure 7 and 8). Now, at this stage a big part of the air was trapped, the air being confined in isolated pores.

In the literature, the second evoked cause is the development of osmotic pressure in the concrete/cover interface. In the case of stiff covers, the developed osmotic pressures can approach the resistance offered by the interface. The osmotic pressures thus seem to be at the origin of the blistering phenomenon of the organic covers applied to concrete. One of the aspects which still remains to be studied is - which is the constituent which plays the role of semipermeable membrane for the soluble salts present in concrete? The answer to this question would doubtlessly allow developing devices to avoid blistering.

7. References

1. Ignoul S., Van Rickstal F., Van Gemert D., Blistering of Epoxy Industrial Floors on concrete substrate : phenomena and case study, *International Conference on Polymers in Concrete*, Berlin (2004)

2. Whitacker S., Simultaneous heat mass and momentum transfer in porous media: a theory of drying, *Advances in heat transfer*, **13**, pp. 119-203 (1977)

3. Whitaker S., Flow in porous media III : deformable media, *Transport in Porous Media*, **1**, pp. 127-154 (1986)

4. Mainguy M., Coussy O., Baroghel-Bouny V., Role of air pressure in drying of weakly permeable materials, *ASCE Journal of Engineering Mechanics*, **127**, pp. 582-592 (2001)

5. Van Genuchten M., Th., A closed form equation for predicting the hydraulic conductivity of unsaturated soils, *Soil Science Society American Journal*, **44**, pp. 892-898 (1980)

6. Lockington D., Parlange J.Y., Dux P., Sorptivity and estimation of water penetration into unsaturated concrete, *Materials and Structures*, **32**, pp. 342-347 (1999)

7. Warlow W.J., Pye P.W., Osmosis as a cause of blistering of in situ resin flooring on wet concrete, *Magazine of Concrete Research*, **30**, pp. 152-156 (1978)

8. Acknowledgements

This study was sponsored by the Matériaux Ingénierie Group which is gratefully acknowledged.